2014 14th International Conference on Control, Automation and Systems (ICCAS 2014)
Oct. 22–25, 2014 in KINTEX, Gyeonggi-do, Korea

# Vision-Based Collaborative Lifting Using Quadrotor UAVs

Suseong Kim[1], Seungwon Choi[1], Hyeonbeom Lee[1] and H.Jin Kim[2*]

[1]Department of Mechanical and Aerospace Engineering, Seoul National University,
Seoul 151-742, Korea (suseongkim, cso103, koreaner33@snu.ac.kr)
[2]Department of Mechanical and Aerospace Engineering, Seoul National University,
Seoul 151-742, Korea (hjinkim@snu.ac.kr) * Corresponding author

**Abstract:** This paper presents vision-based lifting of a payload using two quadrotor UAVs. It is assumed that the exact position of a payload is not available. Specifically, for multiple UAVs to approach and connect the correct spots on the payload, image-based visual servo (IBVS) is adopted. A sliding mode controller is designed to track reference positions and velocities generated by IBVS. A scenario is designed from taking off to lifting the payload. The proposed methods and settings are validated with an experiment.

**Keywords:** UAV, Visual servoing, Manipulation

## 1. INTRODUCTION

Various vertical take-off and landing (VTOL) UAVs, thanks to their wide operating envelope from position hold to aggressive maneuvers and relatively high payload, are good candidates as a mobile manipulator and transporter. In these applications, it is beneficial to use multiple UAVs for two main advantages: First, multiple UAVs can share heavy payloads that cannot be carried by a single UAV. Another reason is that the better controllability in manipulating a payload. For example, by using more than three UAVs, not only position but also attitude of a payload can be manipulated [4].

However, prior to transporting and manipulating a payload, it needs to connect the UAVs to a desired spot on a payload. Because the accurate position of a payload or the connecting spot is often unavailable, it is important to guide each UAV to the exact spot on the payload and connect to it. In such cases, visual information is helpful.

There are several researches on utilizing VTOL UAVs as a manipulator, including cooperative transport [4], [5], swing-free trajectory design for a suspended payload [6], and time-optimal trajectory generation for grasping a moving target [9]. In addition, various of researches have been conducted for utilizing visual information in UAV control problems, including image-based visual servoing (IBVS) [1], [2], [11], [12] and position-based visual servoing (PBVS) [7], [8].

On the other hand, there are very few researches related on incorporating visual information in manipulation or transport using UAVs. In [13], a helicopter capable of connecting to a cargo with visual information is proposed for delivery, where only one helicopter was concerned in a hardware-in-the-loop test, rather than flight tests.

This research is about lifting a payload by using multiple quadrotor UAVs. It is assumed that the exact position of the connecting spot on a payload is not known. In order to put the connecting spot in the middle of the camera view, IBVS [1], [2] is utilized.

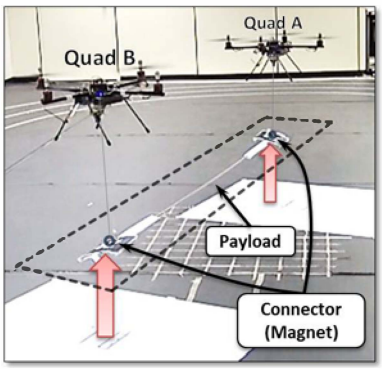


Fig. 1 Two quadrotors lifting a payload collaboratively

## 2. QUADROTOR DYNAMICS

For modeling the quadrotor dynamics, the inertial frame $O_I$ and the body-fixed frame $O_b$ are considered as shown in figure 2. With these coordinate systems, the quadrotor dynamics can be expressed based on the rigid body dynamics as follows:

$$\begin{bmatrix} J\alpha_b \\ ma_I \end{bmatrix} = \begin{bmatrix} \Omega_b \times J\Omega_b + \tau \\ mge_3 + TR_t e_3 \end{bmatrix} \tag{1}$$

where $m$ is the mass of the quadrotor and $J$ is the inertia matrix with respect to the body-fixed frame. In this paper, the reference frame of a quantity is represented with subscripts $I$ and $b$. $\alpha$ and $a$ are angular and translational acceleration respectively, and $R_t$ is the coordinate transformation matrix from $O_b$ to $O_I$. $\Omega$ is the angular velocity of the quadrotor, and $g$ is the gravitational acceleration. The unit vector $e_3$ is $[0\ 0\ 1]^T$. $T$ and $\tau = [\tau_{b,x}\ \tau_{b,y}\ \tau_{b,z}]^T$ are external force and torques from the thrusts generated by the four motors. $T$ and $\tau$ are related with the thrusts $f_{1,2,3,4}$ as

$$\begin{bmatrix} T \\ \tau_{b,x} \\ \tau_{b,y} \\ \tau_{b,z} \end{bmatrix} = \begin{bmatrix} 1 & 1 & 1 & 1 \\ 0 & L & 0 & -L \\ L & 0 & -L & 0 \\ -\rho & \rho & -\rho & \rho \end{bmatrix} \begin{bmatrix} f_1 \\ f_2 \\ f_3 \\ f_4 \end{bmatrix} \tag{2}$$

978-89-93215-06-9 95560/14/$15 

Here, $L$ is the arm length of the quadrotor and $\rho$ is the force-to-moment scaling factor.

Assuming that the quadrotor is in near hover flight condition, the angular velocity $\Omega$ can be considered as very small, and $\Omega = \dot{\Phi}$ where $\Phi = [\phi_I \ \theta_I \ \psi_I]^T$ is the Euler angle of the quadrotor. With the above assumptions, the dynamic equation (1) is simplified as

$$J\ddot{\Phi} = \tau \quad (3)$$

$$ma_I = mge_3 + TR_te_3. \quad (4)$$

Because the quadrotor is an under-actuated system with only four control channels, the dynamics of the quadrotor is considered as two parts. The first part has the states directly controlled by the external force $T$ and torque $\tau$. On the other hand, the states $x_I$ and $y_I$ in the second parts are dependent on the states in the first part of the dynamics. The first part of the dynamics is

$$\ddot{X}_1 = \begin{bmatrix} g \\ 0_{3\times1} \end{bmatrix} + \begin{bmatrix} \frac{1}{m}R_t(3,3) & 0_{1\times3} \\ 0_{3\times1} & J^{-1} \end{bmatrix} \begin{bmatrix} T \\ \tau \end{bmatrix} = F_1 + G_1(X_1)u_1 \quad (5)$$

where $X_1 = [z_I \ \phi_I \ \theta_I \ \psi_I]^T$. Numbers in the parenthesis indicate the location of the element in the corresponding matrix. The dynamics of the second part is

$$\ddot{X}_2 = \frac{T}{m} \begin{bmatrix} \cos\psi_I & \sin\psi_I \\ \sin\psi_I & -\cos\psi_I \end{bmatrix} \begin{bmatrix} \theta_I \\ \phi_I \end{bmatrix} = G_2(X_1)u_2 \quad (6)$$

with the small $\phi_I$ and $\theta_I$ angle assumption, and $X_2 = [x_I \ y_I]^T$.

## 3. IMAGE BASED VISUAL SERVOING

This section briefly explains the relationship between the moving camera coordinate frame and a static point with the calibrated pinhole camera model. After that, IBVS for the quadrotor is presented.

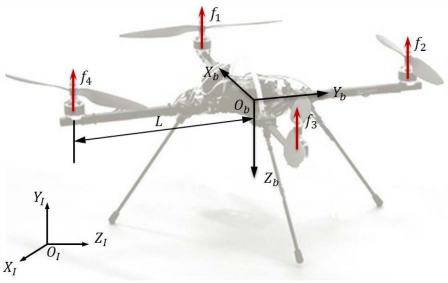


Fig. 2 Coordinates for quadrotor dynamics.

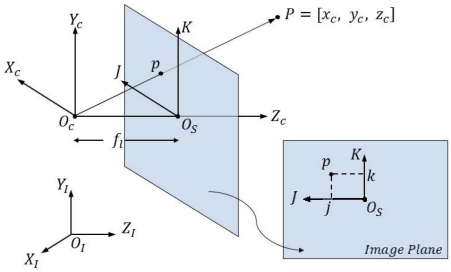


Fig. 3 Camera frame and its image plane.

The configuration of the coordinate system is expressed in fig. 3. The position of the feature point $[j, k]$ on the image plane can be calculated as follows:

$$p = [j, k] = \left[ \frac{f_l x_c}{z_c}, \frac{f_l y_c}{z_c} \right] \quad (7)$$

where $f_l$ denotes focal length and $[x_c, y_c, z_c]$ denotes the position of $P$ with respect to the camera frame.

Let the camera frame move with translational velocity $t = [t_x, t_y, t_z]^T$ and angular velocity $\omega = [\omega_x, \omega_y, \omega_z]^T$, then the dynamics of the point $P$ with respect to the camera frame can be expressed as

$$\dot{P} = -\omega \times P - t \quad (8)$$

By combining (7) and (8), the dynamics of a feature point on the image plane can be derived as

$$\dot{p} = J_p\dot{r} \quad (9)$$

where

$$J_p = \begin{bmatrix} -\frac{f_l}{z_c} & 0 & \frac{j}{z_c} & \frac{jk}{f_l} & -\frac{f_l^2+j^2}{f_l} & k \\ 0 & -\frac{f_l}{z_c} & \frac{k}{z_c} & \frac{f_l^2+k^2}{f_l} & -\frac{jk}{f_l} & -j \end{bmatrix}.$$

and $\dot{r} = [t^T, \omega^T]^T$. $J_p$ is the image Jacobian matrix and it maps the camera velocity vector $\dot{r}$ to the feature point velocity vector $\dot{p}$ in the image plane. IBVS generates velocity references for fully-actuated systems. However, the quadrotor is an under-actuated system and the task of IBVS is to generate translational velocity references for controlling the quadrotor to the desired position and yaw. To realize this, instead of using the positions of the feature points $[j, k]$ directly, roll- and pitch-compensated positions of the feature points are used as follows:

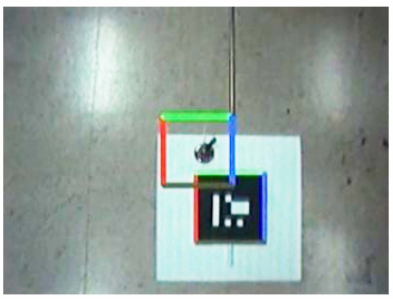

Fig. 4 Tracking four corners using a fiducial marker. The square in the middle is the desired position of the fiducial marker in the image.

$$P^v = R(\phi)R(\theta)P = [x_c^v \ y_c^v \ z_c^v]^T \quad (10)$$

$$p^v = \frac{f_l}{z_c^v} \begin{bmatrix} x_c^v \\ y_c^v \end{bmatrix} = \begin{bmatrix} j^v \\ k^v \end{bmatrix} \quad (11)$$

where the superscript $v$ means roll- and pitch-compensated virtual coordinate frame, and $R(\phi)$ and $R(\theta)$ are roll and pitch rotation matrices, respectively.

The objective of IBVS is to minimize the distances between the desired location of features $p^*$ and actual location of visual features $p^v$ on the image plane.

$$e = p^v - p^* \tag{12}$$

In this paper, visual features are chosen as the four corner points of a square. Because the desired locations of the corner points are stationary,

$$\dot{e} = \dot{p}^v = J_{p^v}\dot{r} \tag{13}$$

To minimize the error, the velocity vector $\dot{r}$ can be set as

$$\dot{r} = -WJ_{p^v}^T e \tag{14}$$

where $W$ is a positive definite matrix. The stability of the error defined in eq. (12) can be easily shown as in [1].

# 4. CONTROLLER DESIGN

This section describes the control design of the quadrotor. The overall control scheme is summarized in fig. 5.

## 4.1 Altitude and Altitude Control

As explained in section 2, the dynamics of the quadrotor is divided into two subsystems. To control the first subsystem given by eq. (5), the sliding surface is defined as

$$S_1 = \dot{e}_1 + C_1 e_1 + C_2 \int e_1 dt \tag{15}$$

where $e = X_1 - X_{1,d}$. $X_{1,d}$ is the vector of desired states and $C_1$ and $C_2$ are diagonal matrices with positive entries. By using the sliding surface, the control law to track the desired attitude and altitude can be derived as the following :

$$u_1 = G_1^{-1}(-F_1 - C_1\dot{e}_1 - C_2 e_1 - C_3 S_1) \tag{16}$$

where $C_3$ is a diagonal matrix with positive entries. The stability of the proposed controller can be proved as the following:

**Proof.** Let Lyapunov candidate function be

$$V_1 = \frac{1}{2}S_1^T S_1 > 0 \tag{17}$$

then under the proposed control law,

$$\dot{V}_1 = -S_1^T C_3 S_1 < 0. \quad \natural \tag{18}$$

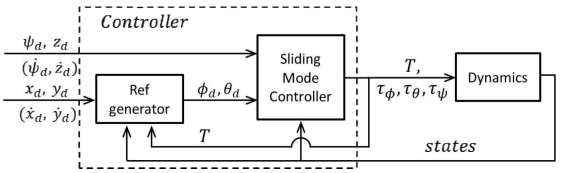


Fig. 5 Structure of the controller

## 4.2 Roll and Pitch Guidance Law

In this subsection, the roll and pitch guidance law to control $[x_I, y_I]$ or $[\dot{x}_I, \dot{y}_I]$ is explained. When the quadrotor is in the normal flight mode, it has to track its position based on the position reference. On the other hand, when the quadrotor is in the IBVS mode, it needs to follow the desired velocity generated with visual information. The guidance law to satisfy both conditions is proposed here.

In the second part of the quadrotor dynamics described in eq. (6), if $\phi_I$ and $\theta_I$ can be controlled accurately, it is possible to utilize the term $u_2$ like a control input. Here, the sliding surface for the second subsystem is defined as

$$S_2 = \dot{e}_2 + C_4 e_2 \tag{19}$$

where $e_2 = [x_I\ y_I]^T - [x_{I,d}\ y_{I,d}]^T$ and $C_4$ is a positive definite matrix. In the position tracking mode, $e_2$ is the position error and $\dot{e}_2$ is set as the corresponding velocity error. In the IBVS mode, $\dot{e}_2$ is the velocity error with respect to the desired velocity command from IBVS, and $e_2$ is computed as the integration of the velocity error.

The suggested control law for $X_2$ is the following:

$$u_2 = G_2^{-1}([\ddot{x}_{1,d}\ \ddot{y}_{1,d}]^T - C_4\dot{e}_{xy} - C_5 S_2) \tag{20}$$

where $C_4$ and $C_5$ are positive definite matrices with positive entries. Stability analysis is summarized in the following:

**Proof.** For the Lyapunov candidate function

$$V_2 = \frac{1}{2}S_2^T S_2 > 0, \tag{21}$$

if the suggested guidance law is substituted, then

$$\dot{V}_2 = -S_2^T C_5 S_2 < 0. \tag{22}$$

# 5. EXPERIMENTAL SETTING

This section describes hardware configuration and experimental scenario.

## 5.1 Hardware Configuration

Detection of the payload and acquisition of guidance information is done by IBVS described before, using a downward-looking camera installed under each quadrotor and the marker on the ground. Once the quadrotor gets close to the payload, connection with the payload is done by using a pendulum attached to the bottom of each quadrotor with a magnet at its tip. After the payload is connected, the additional weight can affect the stability of the quadrotor, especially on the attitude dynamics. To minimize the side effect, the pendulum is installed as close as possible to the center of mass of the quadrotor.

VICON [14], an indoor positioning system, is used to estimate the position and attitude of the quadrotor. The images taken from the camera are transmitted to ground station via 1.3 GHz wireless video transmitter and receiver. Images are captured at 25 fps. The resolution

of the images is 320×240 pixels and the field of view is about 50 degrees. Positions of four corner points of the square are collected using ARToolkitPlus library [15] with fiducial markers.

To transmit the control signal to the quadrotor, we used Spectrum DX7 transmitters connected with Endurance R/C PCTx to the ground station. The quadrotor used in this paper is the Smart Xcopter [16] whose arm length is 25 cm, height is 20 cm and weight is approximately 1 kg.

### 5.2 Mission Scenario

1. Patrol : In this mode, each quadrotor moves toward the mission area while searching their connecting point. When the target point is captured in the image, each quadrotor switches its mode to IBVS-based guidance.
2. IBVS-Guided Approach : In this mode, the guidance signal is generated by IBVS. After detecting the connecting point, each quadrotor approaches the connecting point until sufficiently close to the desired position. If the target image is lost, the mode switches back to the patrol mode and tries to find the target image again.
3. Connecting Payload : To connect to the payload, quadrotors descend their altitude. Since the pendulum is 50 cm long, quadrotors descend to 50 cm.
4. Lifting : After connecting to the payload, both quadrotors ascend to 90 cm. Their movements should be synchronized so that they start lifting at the same moment. Also, the ascent rate of both quadrotors should be the same. The weights are different before and after payload is picked up, i.e.

$$m = m_q + \frac{1}{2}\mathbf{M}m_p,\ \mathbf{M} = \begin{cases} 0, & \text{Patrol and IBVS Mode} \\ 1, & \text{Connect and Lift Mode} \end{cases}$$

where $m_q$ and $m_p$ are the mass of the quadrotor and payload respectively. The weight of the payload is assumed to be known so that it is reflected in the sliding mode controller. The operation ends with simultaneous landing.

## 6. RESULTS

The proposed collaborative lifting technique using the sliding mode controller integrated with IBVS is validated by an experiment. The results are summarized from fig. 7 to 11. Figures plotting position and attitude histories have numbers between the blue dashed vertical lines. Those numbers indicate the modes in the mission scenario : **(1)** the patrol mode, **(2)** the IBVS-guided approaching mode, and **(2*)** means that the quadrotor is waiting for the other one until it finishes its task. **(3)** indicates the connecting mode. **(4)** and **(5)** denote lifting and landing mode, respectively.

Both quadrotors take off from the place about 1 meter apart from the connecting point. They detect the target points with visual information around 18 sec. From that moment, they enter the IBVS-guided approach mode. Quadrotors A and B finish their IBVS-guided in 9.5 and 15.3 sec, respectively. Quadrotor A holds its position

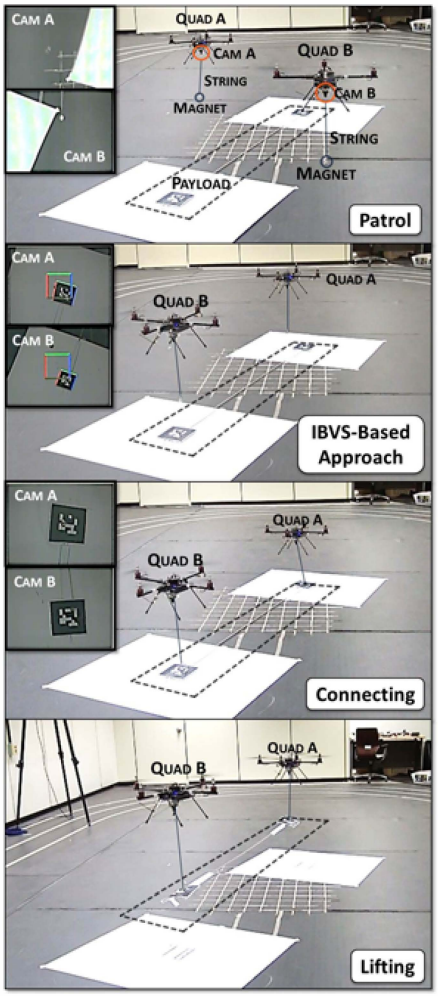


Fig. 6 Snapshots during the experiment showing that both quadrotors carry out their task as designed.

for 5.8 seconds waiting for quadrotor B to finish IBVS-guided approaching. The results of the IBVS-guided approach is summarized in table 1 and fig. 11. Table 1 confirms that both quadrotors approach the designated places with few centimeter errors which are small enough to connect to the payload. Fig. 11 shows that the errors on the image plane are decreased successfully. It is possible because both quadrotors follow the desired velocities generated from IBVS with satisfactory performance as described in fig.10. In fig.10, reference velocities generated from IBVS are low-pass filtered for smoothing before feeding into the sliding mode controller.

After finishing IBVS-guided approaching, both quadrotors decrease their altitude to 0.5 meter to connect to payload. Because their $x$ and $y$ positions were matched close in the previous mode, magnets under the fiducial markers attach to the magnet at the end tip of the pendulum of each quadrotor.

Then, both quadrotors lift a payload collaboratively up to 0.9 meter. The weight of the payload used in the experiment is 300 gram. Since the additional mass is re-

| | Quadrotor | |
|---|---|---|
| | A | B |
| $x_{desired}$ | -0.20 m | 0.40 m |
| $x_{final}$ | -0.17 m | 0.34 m |
| $y_{desired}$ | -0.55 m | 1.15 m |
| $y_{final}$ | -0.54 m | 1.17 m |
| $z_{desired}$ | 0.70 m | 0.70 m |
| $z_{final}$ | 0.62 m | 0.66 m |
| Error | $\approx$ 0.09 m | $\approx$ 0.07 m |

Table 1 Results of IBVS-guided approaching.

flected in the controller, both quadrotors are capable to lift it as desired. Fig. 8 shows that $x$ and $y$ position of both quadrotors are well regulated in the same place even during the lifting.

## 7. CONCLUSION

This paper presented a successful application of two under-actuated quadrotor UAVs for lifting a payload collaboratively. When the position of the payload is not known exactly, UAVs use visual information to approach to the respective connecting points on the payload. IBVS for under-actuated UAV is employed to utilize visual information and it is integrated with a sliding mode controller. This is demonstrated in an experiment with a scenario consisting of multiple stages including take-off, vision-guided approach, connection to the payload, lift, and landing. The experimental results demonstrate that the proposed approach shows satisfactory performance to lift a payload using two UAVs.

## ACKNOWLEDGMENT

This work was supported by the National Research Foundation of Korea(NRF) grant funded by the Ministry of Science, ICT and Future Planning (MSIP) (No. 2009-0083495) and Defense Research Grant, funded by the Agency for Defense Development, under the contract UD120013JD.

## REFERENCES

[1] D. Lee, H. Lim, H. J. Kim, Y. Kim, "Adaptive Image-Based Visual Servoing for an under-actuated Quadrotor System," AIAA Journal of Guidance, Control, and Dynamics, Vol. 35. No. 4. July/August 2012.

[2] D. Lee, T. Ryan and H. J. Kim, "Autonomous Landing of a VTOL UAV on a Moving Platform Using

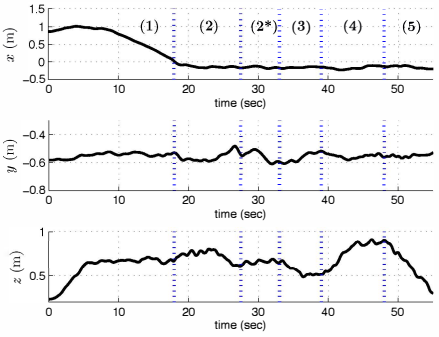


(a)Quadrotor A

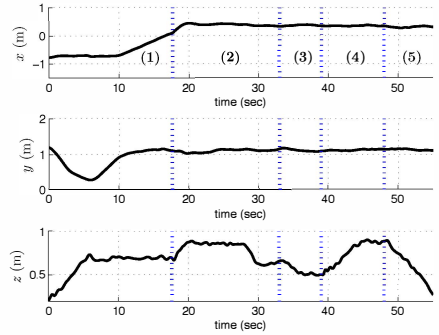


(b)Quadrotor B

Fig. 7 Position history of the quadrotors. **(1)**: Patrol, **(2)**: IBVS-based approach, **(3)**: Connecting payload, **(4)**: Lifting, **(5)**: Landing

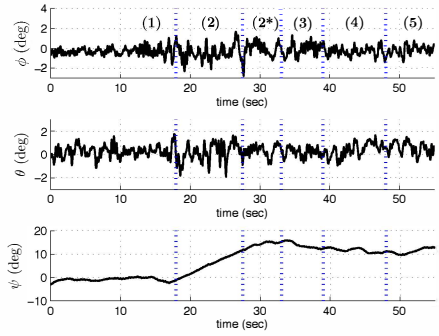


(a)Quadrotor A

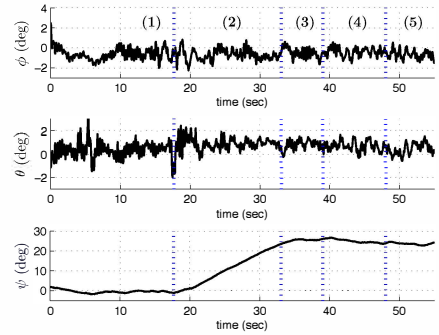


(b)Quadrotor B

Fig. 8 Attitude history of the quadrotors. **(1)**: Patrol, **(2)**: IBVS-based approach, **(3)**: Connecting payload, **(4)**: Lifting, **(5)**: Landing

Image-Based Visual Servoing," IEEE Int. Conf. on Robotics and Automation, pp. 971-976, Minnesota, USA, May 2012.

[3] F. Chaumette and S. Hutchinson, "Visual Servo Control Part1: Basic Approaches," IEEE Robotics and Automation Magazine, Vol. 13, No. 4, pp. 82-90, 2006.

[4] N. Michael, J. Fink, and V. Kumar, "Cooperative Manipulation and Transportation with a Aerial Robots," in Proc. of Robotics: Science and Systems, Seattle, WA, June 2009.

[5] D. Mellinger, M. Shomin, N. Michael, V. Kumar, "Cooperative Grasping and Transport Using Multiple Quadrotors," in Distributed Autonomous Robotic Systems, Lausanne, Switzerland, Nov 2010.

[6] I. Palunko, R. Fierro, and P Cruz, "Trajectory Generation for Swing-Free Maneuvers of a Quadrotor with Suspended Payload: A Dynamic Programming Approach," in IEEE Int. Conf. on Robotics and Automation, RiverCenter, Saint Paul, Minnesota, USA, May 2012.

[7] O. A. Yakimenko, I. I. Kaminer, W. J. Lentz, P. A. Ghyzel, "Unmanned Aircraft Navigation for Shipboard Landing Using Infrared Vision," IEEE Transactions on Aerospace and Electronic Systems, Vol. 38, No. 4, pp. 1191-1200, Oct. 2002.

[8] E. Altug, J. P. Ostrowski, R. Mahony, "Control of a Quadrotor Helicopter Using Visual Feedback," IEEE Int. Conf. on Robotics and Automation, Vol.1, pp. 72-77, Washington DC, USA, May 2002.

[9] R. Spica, A. Franchi, G. Oriolo, H. H. Bülthoff, P R Giordano, "Aerial Grasping of a Moving Traget with a Quadorotor UAV," IEEE/RSJ Int. Conf. on Intelligent Robots and Systems, Vilamoura, Portugal, Oct 2012.

[10] P. Pounds, R. Mahony, P. Corke "Modelling and Control of a Large Quadrotor Robot," Control Engineering Practice, vol. 18, Issue. 7, pp. 691-699, July 2010.

[11] N. Guenard, T. Hamel, R. Mahony, "A Practical Visual Servo Control for a Unmanned Aerial Vehicle," IEEE Transactions on Robotics, vol. 24, Issue. 2, pp. 331-240, April 2008.

[12] T. Hamel, R. Mahony, "Image-Based Visual Servo Control for a Class of Aerial Robotic Systems," Automatica, Vol. 43, No. 11, pp. 1975-1983, Nov 2007.

[13] N. R. Kuntz, P. Y. Oh, "Development of Autonomous Cargo Transport for an Unmanned Aerial Vehicle Using Visual Servoing," ASME Dynamic Systems and Control Conference, An Arbor, Michigan, USA, Oct 2008.

[14] VICON, www.vicon.com

[15] Artoolkitplus, http://studierstube.icg.tugraz.at /handheldar/artoolkitplus.php

[16] Smart Xcopter, http://www.xcopter.com

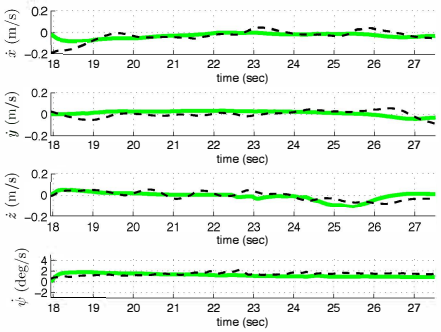


(a)Qaudrotor A

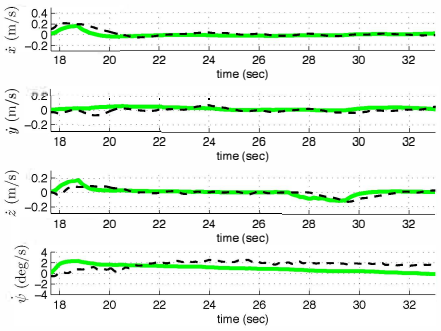


(b)Qaudrotor B

Fig. 9 Velocity history of the quadrotors. Solid-green lines are the reference from IBVS and dashed-black lines the actual velocity.

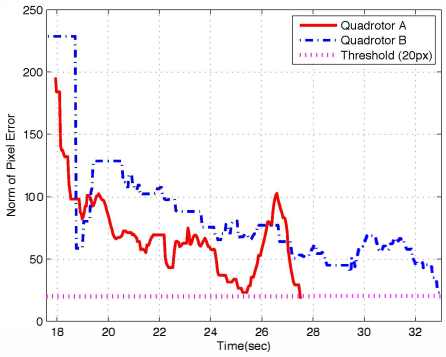


Fig. 10 History of the norm of pixel error, which is the summation of the pixel differences of the four feature points. When the error norm lower than 20, it is considered that the quadrotor is located in the place where the payload can be connected to the quadrotor.